



1 **Strong changes in englacial temperatures despite insignificant changes in ice thickness**
2 **at Dôme du Goûter glacier (Mont-Blanc area)**

3

4 *Christian Vincent¹, Adrien Gilbert¹, Bruno Jourdain¹, Luc Piard¹, Patrick Ginot¹, Vladimir*
5 *Mikhaleenko², Philippe Possenti¹, Emmanuel Le Meur¹, Olivier Laarman¹ and Delphine Six¹*

6

7 *(1) Univ. Grenoble Alpes, CNRS, IRD, Grenoble INP, IGE, 38000 Grenoble, France.*

8 *(2) Institute of Geography, Russian Academy of Sciences*

9

10 **Abstract**

11

12 The response of very high elevation glaciated areas on Mont Blanc to climate change has been
13 analyzed using observations and numerical modeling. Unlike the changes at low elevations, we
14 observe very low glacier thickness changes, of about -2.6 m on the average since 1993. The slight
15 changes in horizontal ice flow velocities and submergence velocities suggest a decrease of about 10 %
16 in ice flux and surface mass balance. This is due to snow accumulation changes and is consistent with
17 the precipitation decrease observed in meteorological data. Conversely, measurements performed in
18 deep boreholes since 1994 reveal strong changes in englacial temperature reaching 1.5 °C at a depth of
19 50 m. We conclude that at such very high elevations, current changes in climate do not lead to visible
20 changes in glacier thickness but cause invisible changes within the glacier in terms of englacial
21 temperatures. Our analysis from numerical modeling shows that glacier near-surface temperature
22 warming is enhanced by increasing melt-frequency at high elevations although the impact on surface
23 mass balance is low. This results in a non-linear response of englacial temperature to currently rising
24 air temperatures. In addition, borehole temperature inversion including a new dataset confirms
25 previous findings of similar air temperature changes at high and low elevations in the Alps.

26

27 **1. Introduction**

28

29 Glaciers are very sensitive to climate change, as shown by numerous studies (e.g. Oerlemans, 2001;
30 Huss, 2012; Thibert et al., 2018). Over recent decades, they have become one of the most emblematic
31 indicators of climate change for the general public. Many glaciers in the world have strongly receded
32 over recent decades (Zemp et al., 2019; Gardner et al., 2013). However, the sensitivity of mass balance
33 to climate can be very different depending on the climatic region and meteorological conditions
34 (Oerlemans, 2001). In addition, the influence of climate change on the surface mass balance depends
35 strongly on elevation (Vincent et al., 2007a). Due to the difficulty of access, very few measurements
36 have been carried out on glaciers at very high elevations (WGMS, 2015) even though englacial



37 temperatures and surface mass balance are amongst the few indicators of climate change at such very
38 high elevations. Englacial temperatures in these cold areas are very sensitive to atmospheric change
39 due the associated increase in surface melting. Gilbert et al. (2014a) showed that the enhanced uptake
40 of energy at the surface of cold glaciers is triggered by the increasing energy flux from the atmosphere
41 due to surface energy balance when surface temperatures reach 0°C. Percolation and refreezing
42 processes efficiently transfer this energy from the surface to underlying layers.

43 In the Alps, most of the observations of mass balance have been carried out on low-altitude glaciers,
44 generally below 3600 m above sea level (a.s.l.) (WGMS, 2015). Most of these glaciers are temperate.
45 Consequently, an increase in surface energy balance leads to an increase in melting. The processes are
46 different for cold glaciers at very high elevations for which an excess of energy balance at the surface
47 results mainly in englacial temperature increase (Hutter, 1983; Aschwanden and Blatter, 2009).

48 Englacial temperature measurements are available for very few cold alpine glaciers at high elevations
49 (Lüthi and Funk, 2000; Suter, 2002; Hoelzle et al., 2011; Vincent et al., 2007b; Gilbert et al., 2010;
50 Gilbert and Vincent, 2013). Even fewer measurements are available at these elevations to
51 simultaneously assess changes in both surface mass balance and englacial temperatures. Our study
52 aims to jointly assess surface mass balance and englacial temperature changes at very high elevation
53 over 25 years (1993-2017) from in-situ measurements at Col du Dôme (4250 m), French Alps, to
54 study the impact of climate change on such high-elevation glaciated areas.

55

56 **2. Study site and data**

57

58 The Dôme du Goûter is located in the Mont Blanc area at an elevation of 4300 m a.s.l, 7 km from
59 Chamonix Mont-Blanc. It is a small ice cap with ice thickness ranging from 45 to 140 m (Vincent et
60 al., 2007b). Three hundred meters from the summit, there is a saddle with very gentle slopes, named
61 Col du Dôme (4250 m a.s.l.). On this saddle, four deep boreholes have been drilled since 1994 at the
62 same location, within a radius of several meters.

63

64 **2.1 Englacial temperature measurements**

65

66 Englacial temperatures were measured from surface to bedrock at the same location (red triangle in
67 Figure 1) using thermistor chains in deep boreholes. Boreholes were drilled electromechanically in
68 1994, 2004 and 2016. The 2010 borehole was drilled using hot water. Thermistors with 0.05 °C
69 accuracy were installed in all boreholes after drilling. In 1994, temperatures were measured 3 days
70 after drilling. In 2004, temperatures were measured 5 days after drilling and again 6 months later. In
71 2010 and 2016, temperatures were measured several times during 6 and 7 months respectively after
72 drilling. Except in 1994, measurements were repeated several times in each borehole until a thermal
73 equilibrium (± 0.05 °C) was reached. Indeed, repeated measurements after drilling and after several



74 weeks or months show that the borehole temperatures below 20 m deep are consistent (± 0.05 °C). The
75 accuracy of measurements performed in 1994 is assessed to be better than ± 0.1 °C. Density profiles
76 were measured along the ice cores extracted in 1994 and in 2012. Note that the englacial temperatures
77 have been measured between the surface and 73 m deep only in the borehole of 2012 and are not used
78 in this study.

79

80 **2.2 Ice-flow velocities and geodetic measurements**

81

82 Horizontal velocities have been obtained from the position of the bottom tip of accumulation stakes, 5
83 m long and 10 cm in diameter, considering the tilt and orientation of the stakes (Vincent et al., 2007a).
84 Depending on the accumulation rate, the stakes were buried by snow every 6 months or every year.
85 Twenty stakes were set up in 1997 (Fig. 1). These stakes were replaced only in 1998, 1999, 2002,
86 2003, 2004, 2008, 2009 and 2016. Consequently, the series of ice-flow velocities and accumulation
87 measurements are not continuous in time. In addition, the stake locations were modified over the
88 period 1997-2004 (Vincent et al., 2007a). From 2009 to 2017, a fixed network of 12 stakes was used,
89 with the stakes always at the same locations, however the measurements were not continuous over this
90 period. The ice-flow velocities have been calculated and averaged over 3 time periods (1997-2004,
91 2009-2011, 2016-2017). The theolodite-based field methods used to obtain surface velocity and
92 surface topography data before 2000 have been fully described by Vincent et al. (1997). After 2000,
93 geodetic measurements were performed with a Leica 1200 Differential GPS (DGPS) unit running with
94 dual frequencies. Occupation times were typically 1 min with 1-s sampling and the number of visible
95 satellites (NAVSTAR and GLONAS) was greater than seven. The distance between the fixed receiver
96 and the mobile receiver was less than 500 m. The DGPS positions have an intrinsic accuracy of ± 0.01
97 m. However, because of the slope and creep of snow, some stakes tilt with time and, depending on the
98 tilt of the stakes (generally less than 10°), the stake horizontal and vertical positions have a maximum
99 uncertainty of ± 0.88 m and ± 0.09 m respectively. Provided that the initial position of the stake is
100 almost vertical ($\pm 3^\circ$), the uncertainty on horizontal and vertical displacement is assumed to be less
101 than 1 m and 0.1 m respectively. The uncertainties of classical topographic measurements before 1995
102 are similar to those of DGPS measurements. The Digital Elevation Models (DEM) were obtained in
103 1993 and 2017 using the same in-situ geodetic methods with a grid size of 30 m. The uncertainty
104 obtained for each measured point of the DEM is ± 0.10 m and depends mainly on the roughness of the
105 surface. In addition, glacier thickness changes were measured along a longitudinal cross section over a
106 distance of about 600 m in June 1993, May 1998, October 2003, September 2009, March 2012 and
107 August 2016 in order to estimate thickness changes over this profile (red line in Figure 1).

108

109 **2.3 Ground Penetrating Radar (GPR) measurements**

110



111 Radio echo soundings were made in June 1993 and completed in 1999 on the Dôme du Goûter ice cap
112 along 12 profiles in order to determine the bedrock topography (Vincent et al., 1997; S. Suter,
113 unpublished data, 1999). The measurements were performed using a pulse radar transmitter (Icefield
114 Instruments, Canada) based on the Narod transmitter (Narod and Clarke, 1994) with a frequency of 5
115 MHz. The speed of electromagnetic wave propagation in the ice was assumed to be identical to the
116 value of $175 \mu\text{s}^{-1}$ found at Colle Gnifetti (Wagner, 1994). The field measurements were performed in
117 such a way as to obtain reflections from the glacier bed located in a vertical plane with the
118 measurement points at the glacier surface. This makes it possible to locate the glacier bed in 2
119 dimensions. The bedrock topography was obtained from envelopes of all ellipse functions giving all
120 the possible reflection positions. The ice thickness in this area ranges from 45 m (Dôme du Goûter) to
121 140 m (Fig.1).

122

123 3. Results

124

125 3.1 Surface elevation changes

126

127 Glacier surface elevation changes were obtained between 1993 and 2017 from DEM comparisons over
128 a surface area of 0.12 km^2 . As can be seen in Figure 2, the thickness changes are not uniform, showing
129 both positive and negative values depending on the location on the glacier. In any case, the changes
130 are small everywhere and do not exceed 7 m between 1993 and 2017. Maximum thinning is located
131 between the summit of Dôme du Goûter and the pass (Col du Dôme). Conversely, the thickness
132 change is slightly positive in south-east of this region. Note that the 1 m increase over 24 years found
133 in this region is small in comparison to annual accumulation which can reach 8 m of snow per year at
134 some sites and in comparison to interannual accumulation variability which can reach more than 2 m
135 of snow per year. The average 1993-2017 thickness change obtained over the entire surface area is -
136 2.65 m.

137 In addition, geodetic measurements were carried out along a longitudinal cross section for different
138 years (Fig. 3). The measurements were not performed during the same season each year but this is not
139 crucial given that melting is close to zero at this altitude (Gilbert et al., 2014a) and snow accumulation
140 occurs throughout the year (Vincent et al., 2007a). Although the measurements were performed on one
141 longitudinal cross section only, it seems that thickness changes over each period of 5 years are as large
142 as changes over the whole period of 24 years. From these data, we can conclude that the thickness
143 changes observed at this altitude over 24 years are very small.

144

145 3.2 Ice flow velocity changes

146



147 Ice flow velocities were measured at numerous locations before 2009 but not always at the same
148 locations (Fig. 4). Conversely, after 2009, the number of stakes was reduced but the stakes were
149 always set up at the same locations. Thanks to the numerous measurements performed between 1997
150 and 2004, the ice flow velocities have been interpolated over the whole colored area shown in Figure
151 4. In this way, we can accurately compare the ice flow velocities over three periods, 1997-2004, 2009-
152 2011 and 2016-2017 at the same locations, i.e. the locations of stakes set up in 2009 and 2016. No
153 significant change in horizontal ice flow velocities can be detected between the 1997-2004 and 2009-
154 2011 periods given that the differences are within the uncertainty of measurements (Fig. 5). Between
155 the 1997-2004 and 2009-2011 periods, the differences are less than 0.86 m a^{-1} except for one point
156 (1.00 m a^{-1}). The average of the differences is 0.05 m a^{-1} and the standard deviation is 0.52 m a^{-1} .
157 Between the 2009-2011 and 2016-2017 periods, the differences are less than 1 m a^{-1} except for 4
158 points (1.1 and 1.09 m a^{-1}). The average of the differences is -0.56 m a^{-1} and the standard deviation is
159 0.43 m a^{-1} . Although these differences barely exceed the measurement uncertainty, they are
160 systematic. Note also that each value results from 3 to 5 topographic surveys, except for the 2016-
161 2017 period. Therefore, these differences observed between the 2009-2011 and 2016-2017 periods
162 could indicate a deceleration over the last decade. The slope of the regression line between ice-flow
163 velocities of the 2009-2011 and 2016-2017 periods is 0.92, which means that the ice flow velocity
164 decreased by 8 %. Over the whole period, using the same method, the ice flow velocity decreased by
165 11 %. One can conclude that the ice flow velocity changes indicate a change in ice flux very likely
166 related to surface mass balance changes. Unfortunately, the surface mass balance measurements are
167 discontinuous. They do not make it possible to detect any temporal change. However, the
168 submergence velocities can help us to analyze the surface mass balance changes as shown in the next
169 section.

170

171

172 3.3 Submergence velocity changes

173

174 The mean surface mass balance can be analyzed indirectly from the submergence velocities. Previous
175 studies (Vincent et al., 2007a), have shown that the submergence velocities appear to offer a good way
176 of assessing the long-term average surface mass balance. Submergence velocities w_s were calculated
177 from:

$$178 w_s = w - u \tan \alpha \quad (1)$$

179

180 where u and w are the measured horizontal and vertical components of the surface velocity obtained
181 from stake measurements and $\tan \alpha$ is the surface slope (Hooke, 2005; Cuffey and Paterson, 2010). The
182 submergence velocities are expressed in meter water equivalent per year (m w.e. a^{-1}) calculated using



183 the density of the firm. Assuming an uncertainty of ± 0.05 for the relative density and ± 0.1 m for the
184 vertical velocity component, the uncertainty should not exceed $0.4 \text{ m w.e. a}^{-1}$.

185 As in the analysis of the horizontal ice flow velocities, the submergence velocities of the 1997-2004
186 period have been interpolated over the whole colored area shown in Figure 6. The submergence
187 velocities can vary from 0.3 to $3.3 \text{ m w.e. a}^{-1}$ depending on the location. This pattern is highly
188 correlated with the accumulation pattern as shown by Vincent et al. (2007a). The submergence
189 velocities have been compared over the three periods 1997-2004, 2009-2011 and 2016-2017 (Fig. 7).
190 The comparison reveals a decrease of the submergence velocities after 2004. Based on the slope of the
191 regression lines, the submergence velocities decreased by 8 % between the 1997-2004 and 2009-2011
192 periods and by 10 % between the 2009-2011 and 2016-2017 periods. Between the 2009-2011 and
193 2016-2017 periods, the average of the differences is $-0.14 \text{ m w.e. a}^{-1}$ and the standard deviation is 0.33
194 m w.e. a^{-1} . Over the whole period (1997-2004 / 2016-2017), the average of the differences is -0.41
195 m w.e. a^{-1} and the standard deviation is $0.21 \text{ m w.e. a}^{-1}$. Although the average difference is close to the
196 uncertainty, the differences are systematic. According to the slope of the regression line, the
197 submergence velocities decreased by 21 % over the whole period. Although the uncertainty is high,
198 these results indicate a decrease of surface mass balances over the whole period. This explains the
199 decrease in ice flow velocities and ice flux. These relative changes in ice flow velocities, ice flux and
200 surface mass balances are thoroughly discussed in section 4.

201

202 3.4 Englacial temperature changes

203

204 Englacial temperature were measured down to the bedrock at the same location between 1994 and
205 2017 during four drilling campaigns (Fig. 8). Measurements reveal a strong warming of near-surface
206 temperatures that likely started before 1994 given that the 1994 temperature profile was already far
207 from steady state conditions (Vincent et al., 2007a). We defined the near-surface temperature as the 10
208 m deep averaged temperature. The near-surface firn temperatures depend on complex mass and energy
209 exchanges at the snow surface but are mainly driven by air temperature and meltwater refreezing. This
210 near-surface temperature anomaly due to atmospheric warming was propagated down to the glacier
211 bottom through advective and diffusive processes throughout the measurement period as shown in
212 Figure 8.

213 Note that between the surface and a depth of 20 m, the englacial temperature is affected by seasonal
214 fluctuations (Gilbert et al., 2014a). At depths between 50 and 55 m, the englacial temperature changes
215 are about $+1.5 \text{ }^\circ\text{C}$ over the whole period (Fig. 8). For the deep layers, below 90 m, the englacial
216 temperature profile does not show any change until after 2005. The warm wave reached the bedrock
217 between 2005 and 2010. Over the whole period (1994-2017), the temperature change close to the
218 bedrock (126 m deep) was $+0.3 \text{ }^\circ\text{C}$, which is larger than the uncertainty of the measurements. Note
219 that the last temperature profile measured in 2017 revealed a stabilization of the 40 m-depth



220 temperature compared to the 2005 and 2010 profiles whereas the temperature anomaly continued to
221 propagate down to the glacier base.

222 From numerical modeling, Gilbert et al. (2014a) showed that near-surface temperature warming can be
223 explained by increasing surface melting event duration. They successfully modeled the temperature
224 evolution up to 2010 using Lyon-Bron meteorological daily data (Météo-France station located 200
225 km west of the glacier) to force their model. The steady state profile was computed from a steady state
226 surface temperature and is used as the initial profile in 1907 for the model. The steady surface
227 temperature was tuned to produce the temperature measured in 1994 (Gilbert and Vincent, 2013). In
228 the present study, we run the same model in order to see if the 40 m-depth temperature stabilization in
229 2017 can be explained by the temperature change and the ensuing increasing frequency and duration
230 of melting events. Results show that the englacial temperature change is still successfully modeled
231 using the same forcing data and parameters (Fig. 8). This means that the 2017 stabilization observed at
232 a depth of 40 m is a signature of an air temperature warming rate slowdown observed in the Lyon-
233 Bron climatic data between 1998 and 2015 and well known on a global scale as “the global warming
234 hiatus” (Meehl et al., 2014). Over the whole temperature profile between 20 and 126 m deep, the
235 average increase in temperature is 0.93 °C between 1994 and 2017. By integrating the internal energy
236 change ($\rho C_p \Delta T$) over the whole glacier thickness, we estimate that the glacier absorbed $3.9 \cdot 10^8 \text{ J m}^{-2}$
237 between the pre-industrial climate (steady state in our simulation) and 2017, where ρ is the firn density
238 (kg m^{-3}), C_p the heat capacity ($\text{J kg}^{-1} \text{ K}^{-1}$) and ΔT the measured temperature change (K). This is
239 equivalent to 1.17 m w.e. of surface melting.

240

241 3.5 Past changes inferred from borehole temperature inversion

242

243 Although it is not the main objective of our study, we compared climate change at Col du Dôme with
244 lower elevation observations, in order to update the findings of Gilbert and Vincent (2013) by
245 including the new temperature profile (measured in 2017) in the inversion procedure. The model is
246 based on Bayesian inference and is fully described in Gilbert and Vincent (2013). The reconstruction
247 of the near-surface temperature at the drilling site (Fig. 9a) includes the four temperature profiles
248 presented here (1994, 2005, 2010 and 2017). It shows a strong and fast change occurring between
249 1980 and 1998 followed by a stabilization or slight cooling until 2015. Near-surface temperatures are
250 estimated to be 2.5 degrees warmer than those in the pre-industrial steady state. The atmospheric
251 temperature reconstruction (Fig. 9b) is based here on the simultaneous inversion of 8 different
252 temperature profiles: the 4 presented here and 4 others from two different locations (Gilbert and
253 Vincent, 2013). The englacial temperature measurements sites are shown in Figure 1. Our analysis
254 confirms that englacial temperature at Col du Dôme showed a break in the warming trend during the
255 early 2000s, similarly to what was observed at lower elevations in the region and at a global scale.

256



257 **4. Discussion**

258

259 The glacier thickness changes observed between 1993 and 2017 are small and non-uniform. Over the
260 whole area, the average thickness has decreased by 2.65 m which corresponds to a reduction of 2.4%
261 of the thickness over this drainage basin (i.e. 2.65/111 m). Note that this thickness change is very
262 small compared to the thickness change of 80 to 100 m observed at low altitudes (about 2000 m a.s.l.)
263 on glaciers in the Mont-Blanc area over the last two decades (Berthier et al., 2014 ; Vincent et al.,
264 2014). At the flux gate shown in Figure 1, the thickness has decreased by 2 % (i.e. 2.56/131 m). Over
265 the same period, the surface horizontal ice flow velocities have decreased by 11 % at this flux gate.
266 Three dimensional modeling with firm specific rheology performed by Gilbert et al. (2014b) shows
267 that the mean horizontal velocity is 70% of the surface horizontal velocity. The mean horizontal
268 velocity of the cross section can therefore be estimated to have decreased by 7.7%. Consequently the
269 ice flux has decreased by about 9.7 % between 1993 and 2017. An independent estimation shows that
270 the submergence velocities have decreased by 21 % over the whole drainage basin. These independent
271 results seem to reveal a slight change in surface mass balance over the whole period. According to the
272 ice flux calculations, the surface mass balance has decreased by about 10 %. The greater change in ice
273 flow velocity compared to the change in thickness is not surprising. Indeed, the glacier is frozen to its
274 bed and no sliding occurs. According to Glen's law and the laminar flow assumption (Cuffey and
275 Paterson, 2010), the relative change in ice thickness is 1/5 of the relative flux change or relative
276 change in surface mass balance, in the absence of large slope changes. Similarly, the relative change in
277 ice flow velocity is 4/5 of the relative change in surface mass balance. Assuming a change of 10 % in
278 surface mass balance, there should be a change of 2 % in ice thickness and 8 % in ice flow velocity.
279 These estimations are consistent with our observations. The ice thickness is therefore not very
280 sensitive to surface mass balance. Conversely, the ice flow velocity is more sensitive and this explains
281 the larger relative changes in ice flow velocities we observed compared to the changes in thickness.

282 The change in surface mass balance we hardly detected could be related to a change in precipitation
283 over the last two decades. Indeed, the surface mass balance at these high elevations is driven by
284 changes in precipitation (Vincent et al., 2007b). We therefore analyzed atmospheric precipitation data
285 from the SAFRAN (Système d'Analyse Fournissant des Renseignements Adaptés à la Nivologie,
286 System of analysis for the provision of information for the science of snow) reanalysis available back
287 to 1958 (Durand et al., 2009) and snow accumulation at lower altitudes from Argentière and Mer de
288 Glace glaciers. This analysis reveals that annual precipitation has decreased by about 10 % in the Mont
289 Blanc area over the last two decades (Fig. 10). The snow accumulation rates observed at Argentière
290 and Mer de Glace glaciers show similar trends although these accumulation rates are related to the
291 winter season only.

292 A source of uncertainty in submergence velocities is related to the snow density. Indeed, the
293 submergence velocity calculations require the snow/firm density values over the depth at which the



294 stakes have been set up. The snow density was not measured for each campaign. For our calculations,
295 we assumed that the snow density did not change with time. The long term change of the firn density
296 was assessed from drilling core measurements from holes drilled in 1994 and 2012 (see
297 Supplementary Material). From these measurements, it seems that the snow density did not change
298 significantly.

299 Over the entire 20th century, a previous study (Vincent et al., 2007b) showed that the thickness of
300 glaciers at these high elevations did not change significantly. It suggested that surface accumulation
301 rates did not change significantly over the entire 20th century although it does not exclude decadal
302 periods with significant accumulation changes. Our results tend to show that the surface mass balance
303 has changed slightly since the beginning of the 21st century. Despite this small change, this glacier can
304 be considered to have been close to steady state conditions over the last 100 years.

305 In opposition to surface mass balance, englacial temperatures are strongly changing in response to
306 atmospheric warming. This highlights the non-linear response of near-surface temperature to
307 atmospheric forcing due a modified surface energy balance when surface melting occurs (Gilbert et
308 al., 2014a). As surface melting events become more and more frequent, the energy absorbed by the
309 glacier is largely enhanced, resulting in a strong warming signal observed in the borehole temperature
310 profiles. Our simulation and inversion shows that the observed temperature profiles reflect a
311 slowdown in the atmospheric warming rate, which is observed at lower elevation at both local and
312 global scales. The slight near-surface temperature cooling trend inferred in our inversion (Fig. 9a) may
313 indicate a negative feedback linked to increasing surface melting that could be superimposed on the
314 atmospheric forcing. Indeed, the increasing refreezing rate could start to create an impermeable ice
315 layer that prevents meltwater percolation and limits its warming effect. With the atmospheric warming
316 rate currently increasing again, future observations will provide the opportunity to evaluate the
317 efficiency of this potential feedback.

318

319

320

321

322

323 **5. Conclusions**

324

325 Our comparison of two Digital Elevation Models produced in 1993 and 2017 over 0.12 km² at Col du
326 Dôme shows that ice thickness changes were very small (<7 m) over this period at this altitude (4250
327 m a.s.l.) in the Mont Blanc area. Ice flow velocity measurements show that the horizontal velocities
328 have decreased by about 11 %. This leads to a decrease in ice flux of 9.7%. Although the surface mass
329 balance observations are not available over the whole period, the ice flux calculations suggest a
330 decrease of surface mass balance. This is confirmed by the analysis of submergence velocities which



331 decreased by 21 % between 1993 and 2017. The overall analysis suggests that surface mass balance
332 might have decreased by about 10 % over this period. Given that ablation is almost negligible
333 compared to snow accumulation (Gilbert et al., 2014a), the change in surface mass balance is likely
334 due to a change in snow accumulation and consequently to a change in precipitation. This is consistent
335 with the meteorological reanalysis and winter snow accumulation measurements performed at lower
336 altitudes.

337 As opposed to thickness and surface mass balance changes, the englacial temperatures reveal strong
338 changes. The englacial temperature averaged over the entire profile increased by 0.9 °C between 1994
339 and 2017. Numerical modeling with meteorological input data shows that the temperature profile was
340 already far from steady state in 1994 in response to a warming phase that started in 1980. The near-
341 surface temperature warming over the last 3 decades propagated down to the glacier and reached the
342 bedrock between 2005 and 2010. Finally, our borehole temperature inversion shows an air temperature
343 change very similar to that observed at low elevations in the Alps, including a warming hiatus
344 occurring during the early 2000's.

345 In the future, near-surface temperature warming should continue to propagate down into the glacier.
346 This warming could affect the stability of cold alpine hanging glaciers located on steep slopes and
347 currently frozen to their bed. The progressive changes in thermal regime of these high elevation
348 glaciers cannot be detected from the surface.

349 For hanging glaciers with basal ice temperatures close to the melting point, ice flow velocity
350 monitoring is recommended, particularly when glacier collapse could jeopardize life and property in
351 the valley below.

352

353 **Data availability:** The englacial temperature data and DEM data can be accessed upon request by
354 contacting Christian Vincent (christian.vincent@univ-grenoble-alpes.fr).

355

356 **Author contributions:** LP, PG, VM, PP, EL drilled the ice cores. OL, DS and CV performed the
357 geophysical and geodetic measurements. AG performed the numerical modeling. CV supervised the
358 study and wrote the paper. All co-authors contributed to discussion of the results.

359

360 **Competing interests:** the authors declare that they have no conflict of interest.

361

362 **Acknowledgements:**

363

364 This study was funded by the AQWA European program and Ice Memory project. 2016 ice coring
365 was conducted with a lightweight ice coring system (<http://cryosphere.co>). We thank Y. Durand, G.
366 Giraud and S. Morin (CNRMGAME/CEN, Meteo France) for providing the SAFRAN data and



367 meteorological data from Lyon-Bron. We would also like to thank everyone who helped in collecting
368 data during the glacier field campaigns including data collected in the framework of GLACIOCLIM
369 program. We are grateful to H. Harder for reviewing the English.

370

371 **References**

372

373 Aschwanden, A., and Blatter, H.: Mathematical modeling and numerical simulation of polythermal
374 glaciers, *J. Geophys. Res.*, 114, F01027, doi:10.1029/2008JF001028, 2009.

375

376 Berthier, E., Vincent, C., Magnússon, E., Gunnlaugsson, Á. Þ., Pitte, P., Le Meur, E., Masiokas, M.,
377 Ruiz, L., Pálsson, F., Belart, J.M.C., and Wagnon, P.: Glacier topography and elevation changes from
378 Pléiades sub-meter stereo images, *The Cryosphere*, 8, 2275–2291, doi:10.5194/tc-8-2275-2014, 2014.

379

380 Cuffey, K., and Paterson, W. B. S.: *The Physics of Glaciers*, 4th ed., Academic, Amsterdam, 2010.

381

382 Durand, Y., Laternser, M., Giraud, G., Etchevers, P., Lesaffre, B., and Mérindol, L.: Reanalysis of 44
383 Yr of Climate in the French Alps (1958–2002): Methodology, Model Validation, Climatology, and
384 Trends for Air Temperature and Precipitation, *J. Appl. Meteorol. Clim.*, 48, 429–449,
385 <https://doi.org/10.1175/2008JAMC1808.1>, 2009.

386

387 Gardner, A.S., Moholdt, G., Cogley, J.G., Wouters, B., Arendt, A.A., Wahr, J., Berthier, E., Pfeffer,
388 T., Kaser, G., Hock, R., Ligtenberg, S.R.M., Bolch, T., Sharp, M., Hagen, J.O., van den Broeke, M.
389 R., and Paul, P.: A reconciled estimate of glacier contributions to sea level rise: 2003–2009, *Science*,
390 340, 6134, 852–857, [https://doi:10.1126/science.1234532](https://doi.org/10.1126/science.1234532), 2013.

391

392 Gilbert, A., Wagnon, P., Vincent, C., Ginot, P., and Funk, M.: Atmospheric warming at a high
393 elevation tropical site revealed by englacial temperatures at Illimani, Bolivia (6340 m above sea level,
394 16°S, 67°W), *J. Geophys. Res.*, 115, D10109, doi:10.1029/2009JD012961, 2010.

395

396 Gilbert, A., and Vincent, C.: Atmospheric temperature changes over the 20th century at very high
397 elevations in the European Alps from englacial temperatures, *Geophys. Res. Lett.*, 40,
398 doi:10.1002/grl.50401, 2013.

399

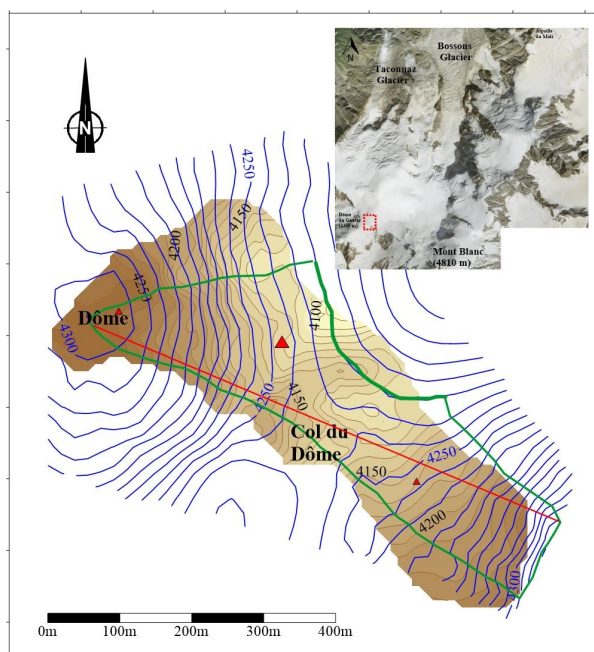
400 Gilbert A., Vincent, C., Six, D., Wagnon, P., Piard, L., and Ginot, P.: Modeling near-surface firn
401 temperature in a cold accumulation zone (Col du Dôme, French Alps): from a physical to a semi-
402 parameterized approach, *The Cryosphere*, 8, 689–703, doi:10.5194/tc-8-689-2014, 2014a.



- 403
- 404 Gilbert, A., Gagliardini, O., Vincent, C., and Wagnon, P.: A 3-D thermal regime model suitable for
405 cold accumulation zones of polythermal mountain glaciers, *J. Geophys. Res.*, 119(9), 1876–1893,
406 doi:10.1002/2014JF003199, 2014b.
- 407
- 408 Hoelzle, M., Darms, G., Lüthi, M.P., and Suter, S.: Evidence of accelerated englacial warming in the
409 Monte Rosa area, Switzerland/Italy, *The Cryosphere*, 5, 231-243, doi:10.5194/tc-5-231-2011, 2011.
- 410
- 411 Hooke, R.L.: *Principles of Glacier Mechanics*, Cambridge University Press, 429 p, 2005.
- 412
- 413 Huss, M.: Extrapolating glacier mass balance to the mountain-range scale: The European Alps 1900-
414 2010. 2012, *The Cryosphere*, 6, 713-727, doi:10.5194/tc-6-713-2012, 2012.
- 415
- 416 Hutter, K.: *Theoretical Glaciology: Material Science of Ice and the Mechanics of Glaciers and Ice*
417 *Sheets*, D. Reidel, Dordrecht, Netherlands, 1983.
- 418
- 419 Lüthi, M., and Funk, M.: Modelling heat flow in a cold, high-altitude glacier: interpretation of
420 measurements from Colle Gnifetti, Swiss Alps, *J. Glaciol.*, 47, 314-324, 2001.
- 421
- 422 Meehl, G. A., Teng, H., and Arblaster, J.M.: Climate model simulations of the observed early-2000s
423 hiatus of global warming, *Nature Climate Change*, 4(10), 898–902, doi:[10.1038/nclimate2357](https://doi.org/10.1038/nclimate2357), 2014.
- 424
- 425 Narod, B.B. and Clarke, G.K.C.: Miniature high-power impulse transmitter for radio-echo sounding. *J.*
426 *Glaciol.*, 40(134), 190-194, 1994.
- 427
- 428 Oerlemans, J.: *Glaciers and Climate change*, Balkema Publishers, Lisse, 2001.
- 429
- 430 Suter, S.: Dépouillement des sondages radar au Col du Dôme, Massif du Mont Blanc, du 1er au 5 juin
431 1993, Travail de stage pratique réalisé sous la responsabilité de M. Funk et de W. Haeberli. Rapport
432 non publié du VAW et de l'EPFZ de Zurich, 1993.
- 433
- 434 Suter, S.: Cold firn and ice in the Monte Rosa and Mont Blanc areas (spatial occurrence, surface energy
435 balance and climatic evidence), Ph.D. thesis, ETH Zurich, 2002.
- 436
- 437 Thibert, E., Dkengne Sielenou, P., Vionnet, V., Eckert, N., and Vincent, C.: Causes of glacier melt
438 extremes in the Alps since 1949, *Geophys. Res. Letters*, 45, <https://doi.org/10.1002/2017GL076333>,
439 2018.



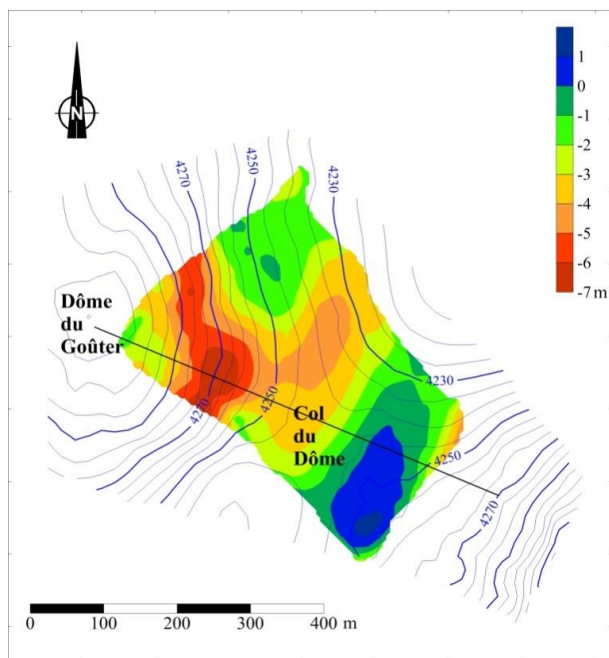
440
441 Vincent, C., Vallon, M., Pinglot, J.F., Funk, M., and Reynaud, L.: Snow accumulation and ice flow at
442 Dôme du Goûter (4300 m), Mont Blanc, French Alps, *J. Glaciol.*, 43, 513-521, Erratum (1998), *J.*
443 *Glaciol.*, 44, 194, 1997.
444
445 Vincent, C., Le Meur, E., Six, D., Funk, M., Hoelzle, M., and Preunkert, S.: Very high elevation Mont
446 Blanc glaciated areas not affected by the 20th century climate change, *J. Geophys. Res.*, 112
447 (D09120), doi:10.1029/2006JD007407, 2007a.
448
449 Vincent, C., Le Meur, E., Six, D., Possenti, P., Lefebvre, E., and Funk, M.: Climate warming revealed
450 by englacial temperatures at Col du Dôme (4250 m, Mont-Blanc area), *Geophys. Res. Lett.*, 34
451 (L16502), doi:10.1029/2007GL029933, 2007b.
452
453 Vincent C., Harter, H., Gilbert, A., Berthier, E., and Six, D.: Future fluctuations of Mer de Glace,
454 French Alps, assessed using a parameterized model calibrated with past thickness changes, *Annals of*
455 *Glaciology*, 55 (66), doi:10.3189/2014AoG66A050, 2014
456
457 Wagner, S.: Dredimensionale modellierung zweier Gletscher und deformations analyse von eisreichem
458 permafrost, PhD thesis, ETH, Zurich, Dissertation 10659, 1994.
459
460 WGMS: Global glacier change bulletin no.1 (2012-2013), Zemp, M., Gärtner-Roer, Nussbaumer, S.
461 U., Hüsler, F., Machgut, H., Mölg, N., Paul, F. and Hoelzle, M. (eds),
462 ICSU(WDS)/IUGG(IASC)/UNEP/UNESCO/WMO, World Glacier Monitoring Service, Zürich,
463 Switzerland, 230 pp, 2015.
464
465 Zemp, M., Huss, M., Thibert, E., Eckert, N., McNabb, R., Huber, J., Barandun, M., Machguth, H.,
466 Nussbaumer, S.U., Gärtner-Roer, I., Thomson, L., Paul, F., Maussion, F., Kutuzov, S., and Cogley,
467 J.G.: Global glacier mass changes and their contributions to sea-level rise from 1961 to 2016,
468 *Nature*, 568, 382–386, doi.org/10.1038/s41586-019-1071-0, 2019.
469



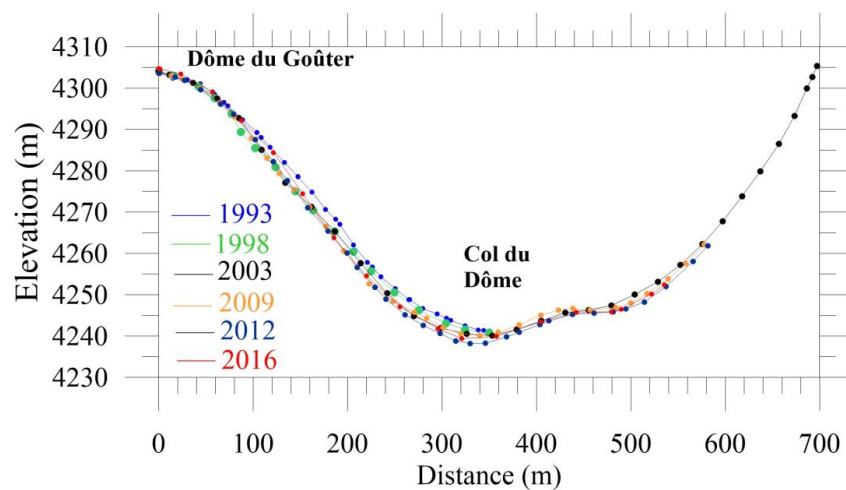
470

471 *Figure 1: Surface (blue) and bedrock (brown) digital elevation models of the Dôme du Goûter area.*
472 *Elevation differences between two contour lines are 5 and 10 m for the surface and bedrock*
473 *respectively. The large red triangle is the location of the core drilling and englacial temperature*
474 *measurement site for this study. The two other small red triangles correspond to the locations of the*
475 *previous englacial temperature measurement sites we used also for the temperature inversion. The*
476 *green line shows the boundaries of the drainage basin and the flux gate (thick line) through which the*
477 *ice flux change has been calculated. The red line shows the cross section used for altitude*
478 *measurements. Aerial picture from Institut Géographique National (©IGN).*

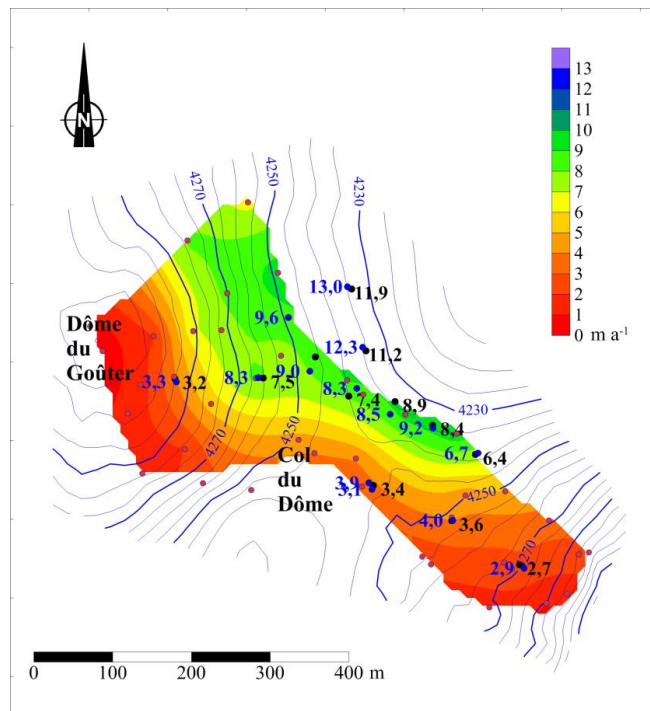
479



480
481 *Figure 2: Thickness changes (color scale) between 1993 and 2017. The contour lines of surface*
482 *topography correspond to the surface of 1993. The longitudinal cross section is shown by the thick*
483 *black line.*
484



485
486 *Figure 3: Longitudinal cross section from Dôme du Goûter to Col du Dôme obtained from DGPS*
487 *measurements performed in June 1993, May 1998, October 2003, September 2009, March 2012 and*
488 *August 2016.*
489



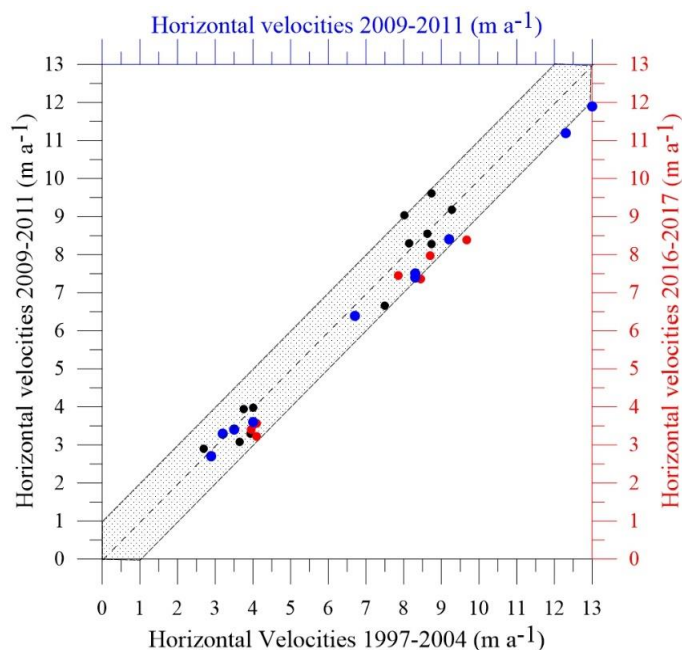
490

491

492 *Figure 4: Horizontal ice flow velocities ($m a^{-1}$) measured between 1993 and 2004 (red dots and color*
493 *scale), between 2009 and 2011 (blue dots and values) and between 2016 and 2017 (black dots and*
494 *values).*

495

496



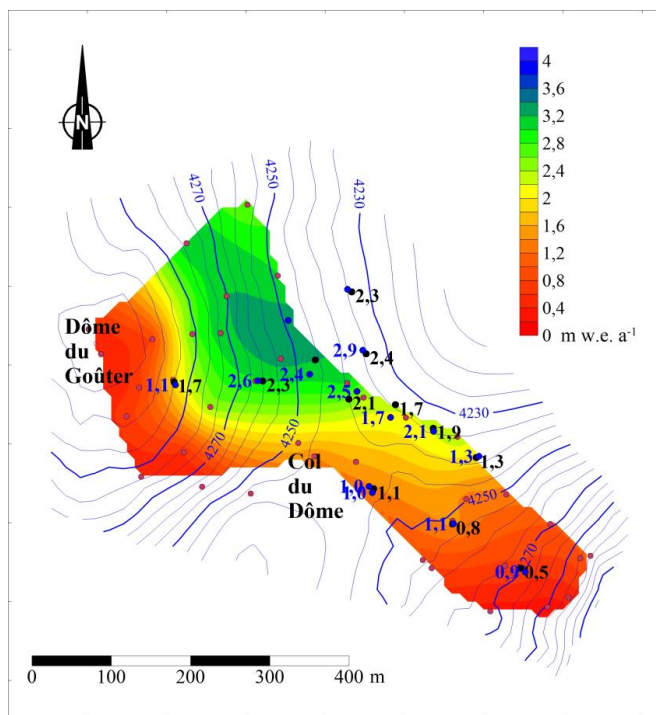
497

498 *Figure 5: Comparison of horizontal ice flow velocities between the periods 1997-2004, 2009-2011 and*
499 *2016-2017. The black dots correspond to the comparison between the 1997-2004 and 2009-2011*
500 *periods. The red dots correspond to the comparison between the 1997-2004 and 2016-2017 periods.*
501 *The blue dots correspond to the comparison between the 2009-2011 and 2016-2017 periods. The gray*
502 *area corresponds to a difference of $\pm 1 \text{ m a}^{-1}$ in relation to the bisector.*

503

504

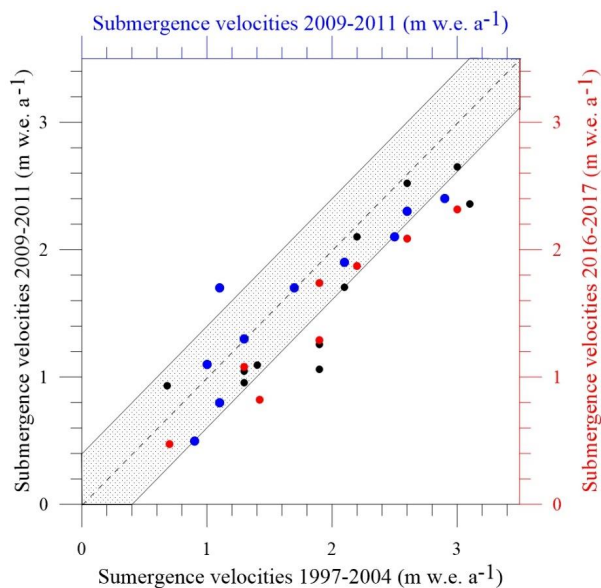
505



506

507 *Figure 6: Submergence velocities (m w.e. a⁻¹) measured between 1997 and 2004 (red dots and color*
508 *scale), between 2009 and 2011 (blue dots and values) and between 2016 and 2017 (black dots and*
509 *values). For the sake of clarity, the submergence velocity values of the 1997-2004 period have not*
510 *been reported here.*

511



512

513 *Figure 7: Comparison of submergence velocities between 1997-2004, 2009-2011 and 2016-2017*

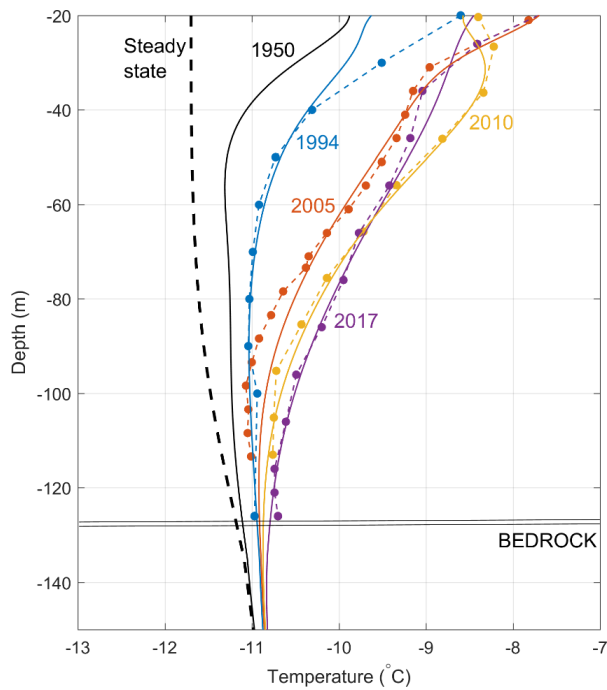
514 *periods. The black dots correspond to the comparison between the 1997-2004 and 2009-2011 periods.*

515 *The red dots correspond to the comparison between the 1997-2004 and 2016-2017 periods. The blue*

516 *dots correspond to the comparison between the 2009-2011 and 2016-2017 periods. The gray area*

517 *corresponds to a difference of ± 0.4 m w.e. a⁻¹ in relation to the bisector.*

518

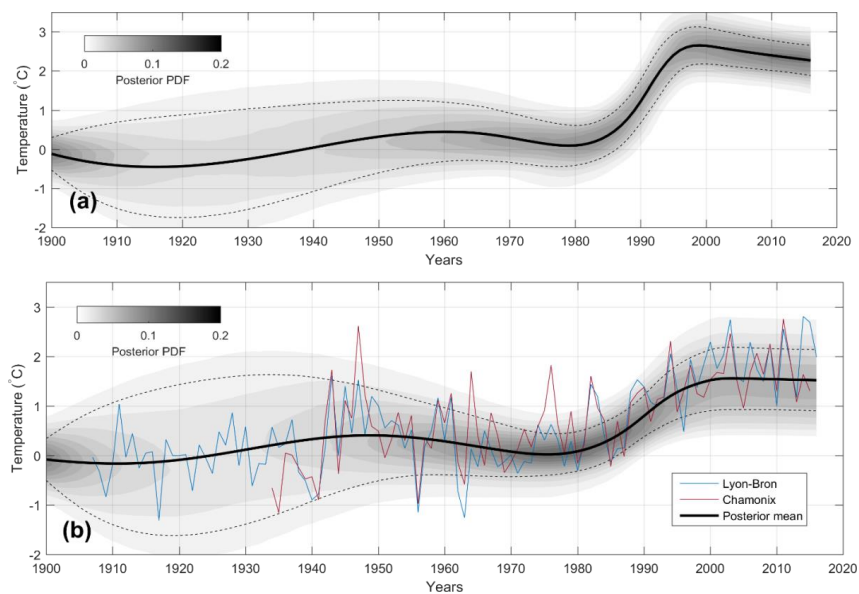


519

520 *Figure 8: Measured (dots) and modeled (continuous lines) englacial temperatures at the same*
521 *location. The model is forced by air temperature data from Lyon-Bron meteorological station, located*
522 *200 km from the drilling site. The steady state profile is computed from a steady surface temperature*
523 *and is used as the initial profile in 1907 for the model.*

524

525



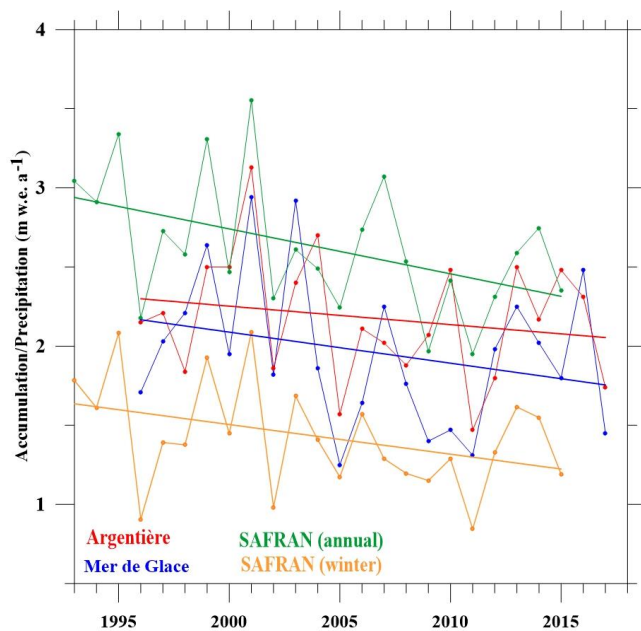
526

527 *Figure 9: (a) Temporal evolution of the near-surface temperature reconstructed at the drilling site*
528 *since 1900 (black bold line). (b) Past atmospheric temperature reconstructed from all measured*
529 *temperature profiles in the Col du Dôme area (black bold line) compared to Lyon-Bron (200 m a.s.l.,*
530 *blue line) and Chamonix (1000 m a.s.l., red line) temperature records. In both plots, the gray scale*
531 *represents the posterior probability function and the dashed line is its standard deviation.*

532

533

534



535

536 *Figure 10: Winter mass balance of Argentière and Mer de Glace glaciers over the period 1995-2017*
537 *and annual/winter precipitation (m w.e.) reanalysis over the period 1993-2015.*

538

539